

Understanding anisotropy generated by fluctuations in heavy-ion collisions

Rajeev S. Bhalerao,¹ Matthew Luzum,² and Jean-Yves Ollitrault³

¹*Department of Theoretical Physics, TIFR, Homi Bhabha Road, Colaba, Mumbai 400 005, India*

²*CEA, IPhT, Institut de physique theorique de Saclay, F-91191 Gif-sur-Yvette, France*

³*CNRS, URA2306, IPhT, Institut de physique theorique de Saclay, F-91191 Gif-sur-Yvette, France*

(Dated: May 29, 2018)

Event-by-event fluctuations are central to the current understanding of ultrarelativistic heavy-ion collisions. In particular, fluctuations in the geometry of the early-time collision system are responsible for new phenomena such as triangular flow, which have solved important puzzles in existing data. We propose a simple model where initial fluctuations stem from independent flux tubes randomly distributed in the transverse plane. We calculate analytically the moments of the initial anisotropies (dipole asymmetry, eccentricity, triangularity), which are the sources of anisotropic flow, and their mutual correlations. Our analytic results are in good agreement with calculations from commonly-used Monte-Carlo codes, providing a simple understanding of the fluctuations contained in these models. Any deviation from these results in future experimental data would thus indicate the presence of non-trivial correlations between the initial flux tubes and/or extra sources of fluctuations that are not present in current models.

PACS numbers: 25.75.Gz, 25.75.Ld, 24.10.Nz

I. INTRODUCTION

Fluctuations of the positions of nucleons within nuclei result in event-by-event fluctuations of the density of matter produced in ultrarelativistic nucleus-nucleus collisions [1–3]. These event-by-event fluctuations have been observed through the centrality and system-size dependence of elliptic flow [4], which is the second Fourier harmonic of the azimuthal distribution of outgoing particles. They may generate elliptic flow even in high-multiplicity proton-proton collisions at the LHC [5, 6], which might be responsible [7, 8] for the near-side ridge observed by CMS [9]. Furthermore, fluctuations result in new, odd harmonics of the azimuthal distribution of outgoing particles, which are clearly seen experimentally through two-particle correlations [10, 11]: The third harmonic, triangular flow [12], is largely responsible for the ridge and away-side structure seen in two-particle correlations and has recently been analyzed at RHIC [13] and LHC [14]. A smaller first harmonic, directed flow [15, 16], is also predicted. Finally, there are non-trivial correlations between these three harmonics [15, 17], and they can be directly measured experimentally [18].

Flow fluctuations are typically studied within Monte-Carlo models of nucleus-nucleus collisions including initial-state fluctuations, such as NeXSPheRIO [19], UrQMD coupled to hydrodynamics [20], EPOS coupled to hydrodynamics [21], AMPT [22, 23], and Glauber models coupled to hydrodynamics [24, 25]. These complex Monte-Carlo approaches do not allow for a simple understanding of the key quantities driving flow fluctuations.

In this paper, we propose a simple model of initial-state fluctuations and, by comparing with full Monte-Carlo calculations, show that it captures the essential physics contained in common models. We assume that the initial energy density profile in the transverse plane

is the superposition of N random independent [26] and identical sources, namely:

$$\epsilon(\vec{x}) = \sum_{j=1}^N \rho(|\vec{x} - \vec{x}_j|), \quad (1)$$

where \vec{x}_j are N independent random variables with a smooth probability distribution $p(\vec{x}_j)$, and $\rho(r)$ is the profile of a single source. The coordinate system is chosen such that centers of colliding nuclei are on the x axis, and the origin lies halfway between the two centers. For a collision of identical nuclei, the system then has the symmetries $p(x, -y) = p(x, y)$ and $p(-x, -y) = p(x, y)$. A standard choice for $\rho(r)$ is a Gaussian profile [24, 25, 27, 28]

$$\rho(r) = \rho_0 e^{-r^2/\sigma^2}, \quad (2)$$

where σ controls the width. The parameters in our model are N , the number of sources, the source distribution $p(\vec{x})$ and the source profile $\rho(r)$.

In Sec. II, we introduce the initial anisotropies ϵ_n and their moments, which are the relevant quantities. We discuss to what extent ϵ_n depends on the source profile $\rho(r)$. In Sec. III, we derive analytic expressions for the rms ϵ_n and compare our results with two Monte-Carlo models. In Sec. IV, our results are extended to higher moments of the distribution of ϵ_n and mixed correlations between harmonics [15, 17, 18].

II. QUANTIFYING INITIAL FLUCTUATIONS

A. Azimuthal asymmetries of the initial distribution

In a given event, the azimuthal distribution of outgoing particles is driven by the azimuthal distribution

of the initial density [27–29]. We define the participant eccentricity [4] ε_2 , the triangularity ε_3 , and the dipole asymmetry [15] ε_1 , and the corresponding orientations Φ_n , by:

$$\begin{aligned}\varepsilon_2 e^{2i\Phi_2} &\equiv -\frac{\{r^2 e^{2i\phi}\}}{\{r^2\}} \\ \varepsilon_3 e^{3i\Phi_3} &\equiv -\frac{\{r^3 e^{3i\phi}\}}{\{r^3\}} \\ \varepsilon_1 e^{i\Phi_1} &\equiv -\frac{\{r^3 e^{i\phi}\}}{\{r^3\}},\end{aligned}\quad (3)$$

where $\{\dots\}$ denotes an average over the transverse plane in a single event, weighted with the energy density:

$$\{f(x, y)\} \equiv \frac{\int f(x, y) \epsilon(x, y) dx dy}{\int \epsilon(x, y) dx dy}, \quad (4)$$

and (r, ϕ) are polar coordinates in which the pole is the center of the distribution, that is, $\{r e^{i\phi}\} = 0$.

The numerators in the right-hand side of Eq. (3) are the cumulants introduced by Teaney and Yan [15]. The anisotropic flow of outgoing particles is driven by these initial anisotropies, in the sense that the relation $v_n \propto \varepsilon_n$ holds approximately [12, 27–30].

B. Dependence of ε_n on source size

Within our simple model, one can easily study the dependence of ε_n on the profile of a single source $\rho(r)$. This is relevant to the early-time dynamics, which has a smearing effect on each source [28] and widens the source profile.

The generating function of cumulants is $W(\vec{k})$, where [15]

$$e^{W(\vec{k})} \equiv \left\{ e^{i\vec{k}\cdot\vec{x}} \right\}. \quad (5)$$

Teaney and Yan's cumulants are obtained by expressing $W(k_x, k_y)$ in terms of $K \equiv k_x + ik_y$ and $\bar{K} \equiv k_x - ik_y$, and expanding in power series of $K^p \bar{K}^q$. Specifically, the numerators of ε_1 , ε_2 and ε_3 in Eq. (3) are obtained by expanding $W(K, \bar{K})$ to order $K\bar{K}^2$, \bar{K}^2 , and \bar{K}^3 , respectively, and $\{r^2\}$ is obtained by expanding $W(K, \bar{K})$ to order $K\bar{K}$.

In our model, Eq. (1), the density profile, is the convolution of the profile of a single source with the distribution of sources $\sum_j \delta(\vec{x} - \vec{x}_j)$. Hence

$$W(\vec{k}) = \ln \left(\frac{\tilde{\rho}(\vec{k})}{\tilde{\rho}(\vec{0})} \right) + \ln \left(\frac{1}{N} \sum_{j=1}^N e^{i\vec{k}\cdot\vec{x}_j} \right), \quad (6)$$

where $\tilde{\rho}(\vec{k})$ is the Fourier transform of the source profile $\rho(r)$. By symmetry, $\tilde{\rho}(\vec{k})$ depends only on $|\vec{k}|^2 = K\bar{K}$. Therefore the numerators of ε_n in Eq. (3) are strictly insensitive to the profile $\rho(r)$. The only dependence of

ε_n on the source profile is contained in the denominator, $\{r^n\}$. If the source has a finite size, $\{r^n\}$ increases, which results in a smearing of anisotropies. One expects that $\{r^n\}$ scales approximately like $\{r^2\}^{n/2}$, resulting in a stronger smearing for ε_3 than for ε_2 , as observed in numerical calculations [28]. One also expects that $\varepsilon_1/\varepsilon_3$ and $\varepsilon_3/\varepsilon_2^{3/2}$ are largely independent of the source profile.

C. Moments

In practice, anisotropic flow is not analyzed in a single event, but in a centrality class. It is inferred from multiparticle azimuthal correlations [31]. To the extent that v_n is driven by ε_n , the measured azimuthal correlations scale like the corresponding moments of the distribution of ε_n and their joint correlations. We introduce the notation [18]:

$$\varepsilon\{n_1, \dots, n_k\} \equiv \langle \varepsilon_{n_1} e^{in_1\Phi_{n_1}} \dots \varepsilon_{n_k} e^{in_k\Phi_{n_k}} \rangle, \quad (7)$$

where angular brackets denote an average over events in a centrality class. With this notation, the rms average of ε_n is

$$\varepsilon_n\{2\} \equiv \langle \varepsilon_n^2 \rangle^{1/2} = \varepsilon\{n, -n\}^{1/2}, \quad (8)$$

where we have used the notation $\varepsilon_n\{2\}$ for the rms value of ε_n [3].

Symmetry with respect to the reaction plane ($y \rightarrow -y$) implies that all moments are real, therefore $\varepsilon\{-n_1, \dots, -n_k\} = \varepsilon\{n_1, \dots, n_k\}$. In addition, $(x, y) \rightarrow (-x, -y)$ symmetry implies that the only nonvanishing moments are those such that $n_1 + \dots + n_k$ is even. Since the azimuthal orientation of each collision is uncontrolled experimentally, one can only measure rotationally symmetric quantities. Thus, the only relevant moments are those satisfying $n_1 + \dots + n_k = 0$. (Some of our intermediate results will involve other moments, such as $\varepsilon\{1, 1\}$ or $\varepsilon\{3, -1\}$.)

Within our independent-source model, all moments can be calculated analytically as a systematic expansion in powers of $1/N$, where N is the number of sources..

III. RMS ASYMMETRIES

The rms value of ε_n is of direct relevance to analyses of anisotropic flow. Indeed, the simplest measurement of anisotropic flow is a pair correlation, $\langle \cos n\Delta\phi \rangle$, which is the average value over events of v_n^2 . Assuming that $v_n \propto \varepsilon_n$ on an event-by-event basis, this scales like $\langle \varepsilon_n^2 \rangle = \varepsilon_n\{2\}^2$. In this Section, we derive analytic results for $\varepsilon_n\{2\}$ within our independent-source model, and compare with numerical results.

A. Analytic results

We denote by $\langle f(x, y) \rangle$ the average value of $f(x, y)$ with the source probability density $p(\vec{x})$, and we introduce the notation $\delta_f \equiv \{f\} - \langle f \rangle$ for the event-by-event fluctuations. We use the complex coordinate $z = x + iy$. The asymmetry ε_n is given by Eq. (3), where we replace $re^{i\phi}$ by $z - \delta_z$ to take into account the recentering correction. To leading order in fluctuations, one obtains

$$\begin{aligned} \varepsilon_3 e^{3i\Phi_3} &= -\frac{\{(z - \delta_z)^3\}}{\{r^3\}} \simeq -\frac{\delta_{z^3} - 3\langle z^2 \rangle \delta_z}{\langle r^3 \rangle} \\ \varepsilon_1 e^{i\Phi_1} &= -\frac{\{(z - \delta_z)^2(\bar{z} - \delta_{\bar{z}})\}}{\{r^3\}} \\ &\simeq -\frac{\delta_{z^2\bar{z}} - 2\langle z\bar{z} \rangle \delta_z - \langle z^2 \rangle \delta_{\bar{z}}}{\langle r^3 \rangle}, \end{aligned} \quad (9)$$

where $\bar{z} = x - iy$. The rms value of ε_n involves an average over events of products of δ 's. Two-point averages are computed using the following identity, which holds for independent sources [26]:

$$\langle \delta_f \delta_g \rangle = \frac{\langle fg \rangle - \langle f \rangle \langle g \rangle}{N}. \quad (10)$$

We thus obtain, using the identities $\langle z^n \bar{z}^m \rangle = 0$ for odd $n - m$ and $\langle z^n \bar{z}^m \rangle = \langle r^{n+m} \cos((n - m)\phi) \rangle$ for even $n - m$:

$$\begin{aligned} \varepsilon_3\{2\}^2 &= \frac{\langle r^6 \rangle + 6\varepsilon_s \langle r^2 \rangle \langle r^4 \cos 2\phi \rangle + 9\varepsilon_s^2 \langle r^2 \rangle^3}{N \langle r^3 \rangle^2} \\ \varepsilon_1\{2\}^2 &= \frac{1}{N \langle r^3 \rangle^2} [\langle r^6 \rangle - 4\langle r^2 \rangle \langle r^4 \rangle + 4\langle r^2 \rangle^3 \\ &\quad + 2\varepsilon_s \langle r^2 \rangle \langle r^4 \cos 2\phi \rangle + 5\varepsilon_s^2 \langle r^2 \rangle^3]. \end{aligned} \quad (11)$$

In these equations, $\varepsilon_s \equiv -\langle r^2 \cos 2\phi \rangle / \langle r^2 \rangle$ denotes the standard eccentricity. We also recall the result for $\varepsilon_2\{2\}$ which has been derived earlier [26].

$$\varepsilon_2\{2\}^2 = \varepsilon_s^2 + \frac{\langle r^4 \rangle (1 + 3\varepsilon_s^2) + 4\varepsilon_s \langle r^4 \cos 2\phi \rangle}{N \langle r^2 \rangle^2}. \quad (12)$$

The first term in the right-hand side is the standard eccentricity, and the second term is the contribution of eccentricity fluctuations to order $1/N$. For a large number of sources, $N \gg 1$, the participant eccentricity ε_2 reduces to the standard eccentricity, while odd harmonics ε_1 and ε_3 vanish.

B. Comparison with Monte-Carlo results

We now compare analytic results derived from our independent-source model with results obtained using the mckt-v1.00 Monte-Carlo [32]. With this Monte-Carlo one can calculate results from both a Color-Glass-Condensate (CGC) inspired model — the MC-KLN [33] improved with running-coupling BK unintegrated gluon densities [34], as well as a standard Monte-Carlo Glauber [35]. We present only results for Pb-Pb collisions at 2.76 TeV per nucleon-nucleon collision,

though results for 200 GeV Au-Au collisions agree equally well. In the Glauber model, each participant nucleon is given a weight [36] $w = 1 - x + xN_{\text{coll}}$, where N_{coll} is the number of binary collisions of that nucleon, and $x = 0.18$ [37].

One input of our model is the probability distribution of sources in the transverse plane, $p(\vec{x})$. For the sake of consistency, we assume that sources are distributed according to the average density profile: $p(\vec{x}) \equiv \langle \varepsilon(\vec{x}) \rangle$, where $\langle \dots \rangle$ denotes an average over many events in a centrality class. We assume pointlike sources for simplicity: $\rho(|\vec{x}|) = \delta(\vec{x})$. The last free parameter in our model is the number of independent sources N . One expects that this number scales typically like the number of participant nucleons in a collision. However, participants are not independent, but strongly correlated: for each participant of the projectile, there is by definition at least one participant from the target which is close enough in the transverse plane for a collision to occur. Nevertheless, it is plausible that the system behaves like a set of N independent clusters of two or more nucleons. Again for simplicity, we use $N = 0.45N_{\text{part}}$ for all centralities, though one could make the agreement with Monte-Carlo even better by fitting N for each centrality class. Increasing N by 20% typically decreases $\varepsilon_3\{2\}$ and $\varepsilon_1\{2\}$ by 10%, and $\varepsilon_2\{2\}$ by less than 4%. If one uses a larger value of N for peripheral collisions (say, $N = 0.6N_{\text{part}}$ instead of $N = 0.45N_{\text{part}}$), agreement with Monte-Carlo is significantly better for $\varepsilon_1\{2\}$ and $\varepsilon_3\{2\}$ but slightly worse for $\varepsilon_2\{2\}$.

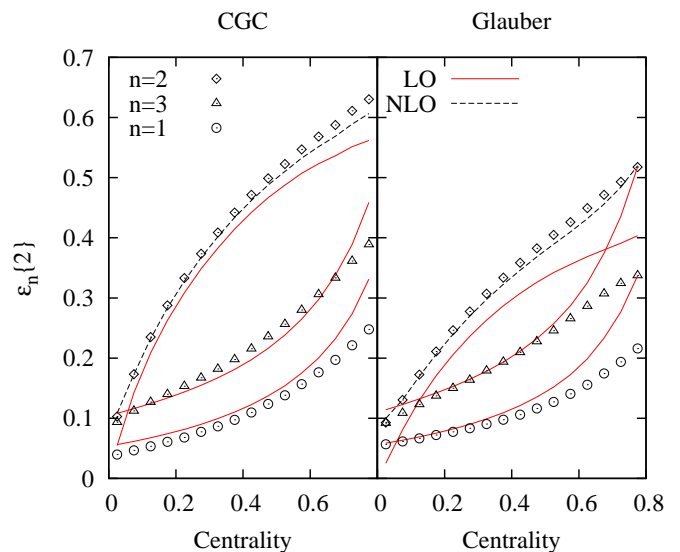


FIG. 1. (Color online) $\varepsilon_n\{2\}$, with $n = 1, 2, 3$, versus centrality. Symbols are Monte-Carlo results, lines are our analytic results for independent sources. For $\varepsilon_2\{2\}$, the dashed line is the full result to order $1/N$ (Eq. (12)), while the solid line is the standard eccentricity (first term in the right-hand side of Eq. (12)).

Fig. 1 displays a comparison between our result (11)

and Monte-Carlo calculations. Our analytic formulae reproduce the centrality dependence of ε_n computed using Monte-Carlo KLN or Monte-Carlo Glauber¹. Odd harmonics, ε_1 and ε_3 , have a mild centrality dependence and essentially scale like $1/\sqrt{N_{\text{part}}}$. On the other hand, ε_2 is much larger for semi-central collisions: this increase is driven by the almond shape of the overlap area between the two nuclei. For ε_2 , we show both the standard eccentricity, which is the leading-order term in a $1/N$ expansion, and the full expression including eccentricity fluctuations to order $1/N$ (Eq. (12)). The standard eccentricity is significantly larger for KLN than for Glauber [39, 40], so that eccentricity fluctuations (which are roughly the same in both models) are a smaller relative correction.

Our model explains why $\varepsilon_1 < \varepsilon_3$, a feature which was observed in Monte-Carlo calculations but yet unexplained. This may be readily understood from Eq. (11) for central collisions, where $\varepsilon_s = 0$: only the $\langle r^6 \rangle$ remains for $\varepsilon_3\{2\}^2$, while $\varepsilon_1\{2\}^2$ has an additional contribution proportional to $\langle r^2 \rangle^2 - \langle r^4 \rangle$, which is negative. For sake of completeness, we have also carried out two other sets of Glauber calculations with only wounded nucleon scaling ($x = 0$) or binary collision scaling ($x = 1$). Values of $\varepsilon_1/\varepsilon_3$ turn out to be significantly smaller for wounded nucleons (between 0.3 and 0.4 for 0-50% centralities) than for binary collisions (between 0.6 and 0.7). This strong ordering is not reproduced by our analytic result, which gives intermediate results (between 0.5 and 0.6 in both cases). We do not have a simple explanation for this discrepancy.

IV. HIGHER-ORDER MOMENTS

A. Fluctuations of ε_n

The ALICE collaboration has recently measured $v_2\{4\}$ [41] and $v_3\{4\}$ [14]. The relative magnitude of $v_n\{4\}$ and $v_n\{2\}$ depends on event-by-event fluctuations of v_n if nonflow effects are small. Assuming that v_n is proportional to ε_n on an event-by-event basis, fluctuations of v_n are due to fluctuations of ε_n :

$$\left(\frac{v_n\{4\}}{v_n\{2\}}\right)^4 = \left(\frac{\varepsilon_n\{4\}}{\varepsilon_n\{2\}}\right)^4 \equiv 2 - \frac{\langle \varepsilon_n^4 \rangle}{\langle \varepsilon_n^2 \rangle^2}, \quad (13)$$

where we have introduced the 4-cumulant $\varepsilon_n\{4\}$ [3]. $v_n\{4\}$ is thus related to $\langle \varepsilon_n^4 \rangle$, which is $\varepsilon\{n, n, -n, -n\}$ in the notation of Eq. (7). Fig. 2 displays the ratio $\langle \varepsilon_n^4 \rangle / \langle \varepsilon_n^2 \rangle^2$ for $n = 1, 2, 3$. The larger the ratio, the larger the fluctuations of ε_n . Note that the order of the curves in Fig. 2 is reversed compared to Fig. 1: smaller values of ε_n go with larger fluctuations. For the most central

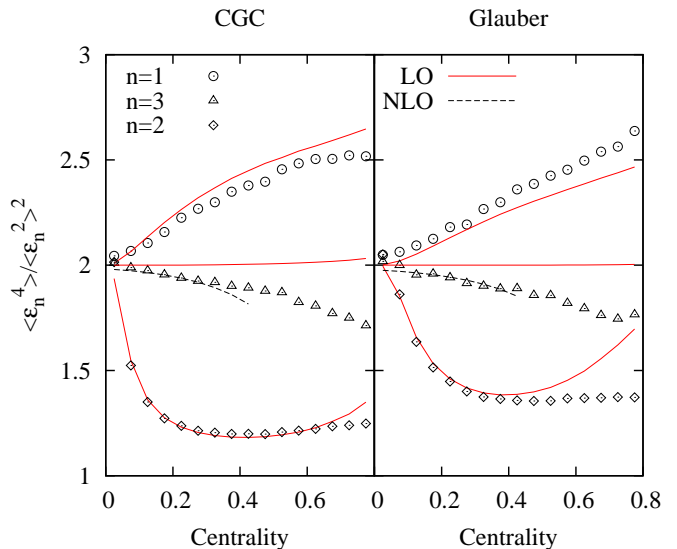


FIG. 2. (Color online) Ratio $\langle \varepsilon_n^4 \rangle / \langle \varepsilon_n^2 \rangle^2$, with $n = 1, 2, 3$, versus centrality. As in Fig. 1, symbols are Monte-Carlo results. Full lines are leading-order analytic results. The dashed line for $n = 3$ includes next-to-leading order corrections derived in Appendix. Although our next-to-leading order result is valid for central collisions only, we compare with Monte-Carlo data up to 40% centrality.

collisions, ratios are close to 2 for all n . This value corresponds to Gaussian fluctuations [42].

For $n = 2$, the ratio quickly decreases with centrality. This is due to the standard eccentricity ε_s , which is zero for central collisions but dominates over eccentricity fluctuations above 10% centrality. The smaller eccentricity fluctuations, the closer the ratio to 1. The decrease is stronger for the KLN model than for the Glauber model because of the larger ε_s . Monte-Carlo results are compared with an analytic result using the expression of $\varepsilon_2\{4\}$ to order $1/N$ derived in [26]. In practice, $\varepsilon_2\{4\} \simeq \varepsilon_s$ for all centralities.

We now compute $\langle \varepsilon_3^4 \rangle$ within our independent-source model. To leading order in the fluctuations, ε_3 is given by Eq. (9), and $\langle \varepsilon_3^4 \rangle$ involves products of four δ 's. To leading order in $1/N$, average values of such products can be expressed in terms of two-point averages (Eq. (10)) using Wick's theorem. For instance, the four-point function is [43]

$$\langle \delta_f \delta_g \delta_h \delta_k \rangle = \langle \delta_f \delta_g \rangle \langle \delta_h \delta_k \rangle + \langle \delta_f \delta_h \rangle \langle \delta_g \delta_k \rangle + \langle \delta_f \delta_k \rangle \langle \delta_g \delta_h \rangle. \quad (14)$$

This identity gives

$$\varepsilon\{3, 3, -3, -3\} = 2\varepsilon\{3, -3\}^2 + \varepsilon\{3, 3\}\varepsilon\{-3, -3\}, \quad (15)$$

or, equivalently,

$$\frac{\langle \varepsilon_3^4 \rangle}{\langle \varepsilon_3^2 \rangle^2} = 2 + \left(\frac{\varepsilon\{3, 3\}}{\varepsilon_3\{2\}^2}\right)^2. \quad (16)$$

¹ We have also done comparisons with the PHOBOS Monte-Carlo Glauber [38], and found that ε_1 from this model is significantly smaller than predicted by our analytic formula.

$\varepsilon\{3, 3\}$ can easily be calculated to order $1/N$ in the same way as $\langle\varepsilon_3^2\rangle$:

$$\begin{aligned}\varepsilon\{3, 3\} &= \langle\varepsilon_3^2 \cos 6\Phi_3\rangle \\ &= \frac{1}{N\langle r^3\rangle^2} (\langle r^6 \cos 6\phi\rangle + 6\varepsilon_s\langle r^2\rangle\langle r^4 \cos 4\phi\rangle \\ &\quad - 9\varepsilon_s^3\langle r^2\rangle^3).\end{aligned}\quad (17)$$

Inserting Eqs. (11) and (17) into (16), we obtain a leading-order analytic result for the ratio. This analytic result is independent of N , and very close to 2 in practice, as can be seen in Fig. 2. This means that the first term on the right-hand side is the dominant contribution [42]. It is easy to understand why the second term is small: $\varepsilon\{3, 3\}$ involves the 6th Fourier harmonic of the initial distribution, which is of order ε_s^3 . Therefore the last term in Eq. (16) is of order ε_s^6 , which is very small in practice.

The Monte-Carlo results in Fig. 2 show that the ratio $\langle\varepsilon_3^4\rangle/\langle\varepsilon_3^2\rangle^2$ is slightly smaller than 2 for both Monte-Carlo KLN and Glauber models (a fact also implied by experimental results [44]), which cannot be explained by our leading-order result Eq. (16). The next-to-leading correction (restricted to central collisions) is derived in the Appendix. It is negative and scales like $1/N$. As shown in Fig. 2, it improves agreement.

Finally, $\langle\varepsilon_1^4\rangle$ can be computed in the same way. The leading-order result is:

$$\frac{\langle\varepsilon_1^4\rangle}{\langle\varepsilon_1^2\rangle^2} = 2 + \left(\frac{\varepsilon\{1, 1\}}{\varepsilon_1\{2\}^2}\right)^2, \quad (18)$$

where

$$\begin{aligned}\varepsilon\{1, 1\} &= \langle\varepsilon_1^2 \cos 2\Phi_1\rangle \\ &= \frac{1}{N\langle r^3\rangle^2} (\langle r^6 \cos 2\phi\rangle - 8\varepsilon_s\langle r^2\rangle^3 + 2\varepsilon_s\langle r^2\rangle\langle r^4\rangle \\ &\quad - 4\langle r^2\rangle\langle r^4 \cos 2\phi\rangle - \varepsilon_s^3\langle r^2\rangle^3).\end{aligned}\quad (19)$$

This quantity is negative, which means that the dipole asymmetry develops mostly out of the reaction plane for non-central collisions. The last term in Eq. (18) gives a positive contribution to the ratio $\langle\varepsilon_1^4\rangle/\langle\varepsilon_1^2\rangle^2$, which increases up to 3 for peripheral collisions. Note that $\varepsilon_1\{4\}$ defined by Eq. (13) is negative, so that $\varepsilon_1\{4\}$ is undefined.

The leading order result defined by Eqs. (18), (11) and (19) is independent of N . It is in good agreement with Monte-Carlo results.

Note that within our independent-source model, the ratios plotted in Fig. 2 are strictly insensitive to the profile of a single source $\rho(r)$.

B. Mixed correlations

We now study the correlations between Φ_1 , Φ_2 and Φ_3 . The lowest order non-trivial correlations are

$$\begin{aligned}\varepsilon_{23} &\equiv \varepsilon\{3, 3, -2, -2, -2\} = \langle\varepsilon_3^2\varepsilon_2^3 \cos(6(\Phi_3 - \Phi_2))\rangle \\ \varepsilon_{12} &\equiv \varepsilon\{1, 1, -2\} = \langle\varepsilon_1^2\varepsilon_2 \cos(2(\Phi_1 - \Phi_2))\rangle\end{aligned}$$

$$\begin{aligned}\varepsilon_{123} &\equiv \varepsilon\{3, -2, -1\} = \langle\varepsilon_3\varepsilon_2\varepsilon_1 \cos(3\Phi_3 - 2\Phi_2 - \Phi_1)\rangle \\ \varepsilon_{1223} &\equiv \varepsilon\{3, 1, -2, -2\} = \langle\varepsilon_1\varepsilon_3\varepsilon_2^2 \cos(3\Phi_3 + \Phi_1 - 4\Phi_2)\rangle \\ \varepsilon_{13} &\equiv \varepsilon\{3, -1, -1, -1\} = \langle\varepsilon_3\varepsilon_1^3 \cos(3(\Phi_3 - \Phi_1))\rangle.\end{aligned}\quad (20)$$

All these correlations were studied numerically in Ref. [18], with the exception of ε_{1223} which is new. We derive an analytic prediction for these quantities using our independent-source model. To leading order in $1/N$, one can replace each factor of $\varepsilon_2 e^{\pm 2i\Phi_2}$ in Eq. (7) by the standard eccentricity ε_s . The moments in Eq. (20) can then be expressed in terms of two-point moments using Wick's theorem:

$$\begin{aligned}\varepsilon\{3, 3, -2, -2, -2\} &= \varepsilon_s^3\varepsilon\{3, 3\} \\ \varepsilon\{1, 1, -2\} &= \varepsilon_s\varepsilon\{1, 1\} \\ \varepsilon\{3, -2, -1\} &= \varepsilon_s\varepsilon\{3, -1\} \\ \varepsilon\{3, 1, -2, -2\} &= \varepsilon_s^2\varepsilon\{3, 1\} \\ \varepsilon\{3, -1, -1, -1\} &= 3\varepsilon\{3, -1\}\varepsilon\{1, 1\}.\end{aligned}\quad (21)$$

To leading order in $1/N$, $\varepsilon\{3, 3\}$ and $\varepsilon\{1, 1\}$ are given by Eqs. (17) and (19). The remaining two-point functions $\varepsilon\{3, -1\}$ and $\varepsilon\{3, 1\}$ can be computed similarly:

$$\begin{aligned}\varepsilon\{3, -1\} &= \langle\varepsilon_3\varepsilon_1 \cos(3\Phi_3 - \Phi_1)\rangle \\ &= \frac{1}{N\langle r^3\rangle^2} (\langle r^6 \cos 2\phi\rangle + 3\varepsilon_s\langle r^2\rangle\langle r^4\rangle \\ &\quad - 6\varepsilon_s\langle r^2\rangle^3 - 3\varepsilon_s^3\langle r^2\rangle^3 - 2\langle r^2\rangle\langle r^4 \cos 2\phi\rangle \\ &\quad + \varepsilon_s\langle r^2\rangle\langle r^4 \cos 4\phi\rangle) \\ \varepsilon\{3, 1\} &= \langle\varepsilon_3\varepsilon_1 \cos(3\Phi_3 + \Phi_1)\rangle \\ &= \frac{1}{N\langle r^3\rangle^2} (\langle r^6 \cos 4\phi\rangle + 4\varepsilon_s\langle r^2\rangle\langle r^4 \cos 2\phi\rangle \\ &\quad - 2\langle r^2\rangle\langle r^4 \cos 4\phi\rangle + 9\varepsilon_s^2\langle r^2\rangle^3).\end{aligned}\quad (22)$$

These equations define our analytic results for the moments.

We now compare our analytic results with Monte-Carlo results. We first scale $\varepsilon\{n_1, \dots, n_k\}$ by $\varepsilon_{n_1}\{2\} \dots \varepsilon_{n_k}\{2\}$ to single out the angular correlation as in Ref. [18]. We compute these ratios both with the Monte-Carlo and with our analytic formulas. To leading order in $1/N$, we use the approximation $\varepsilon_2\{2\} \simeq \varepsilon_s$. One easily shows, using Eq. (21), that the resulting leading-order prediction for the ratios is independent of N .

Fig. 3 displays a comparison between Monte-Carlo results and analytic results. Our leading-order results explain the sign, magnitude, and centrality dependence of all ratios.

The scaled ε_{23} is much smaller than unity, in agreement with earlier observations that triangularity and eccentricity are uncorrelated [20] except for peripheral collisions [45]. One thus expects that triangular flow and elliptic flow are essentially uncorrelated, as confirmed by a recent experimental analysis [14]. Note that while data agree qualitatively with expectations, they do not agree quantitatively with existing Monte-Carlo models [44].

We now discuss the remaining correlations, which involve Φ_1 and are not yet measured. The scaled ε_{13} is large for peripheral collisions, which means that there is a strong positive correlation between $3\Phi_1$ and $3\Phi_3$ [17]. On the other hand, ε_{12} is negative, which means that

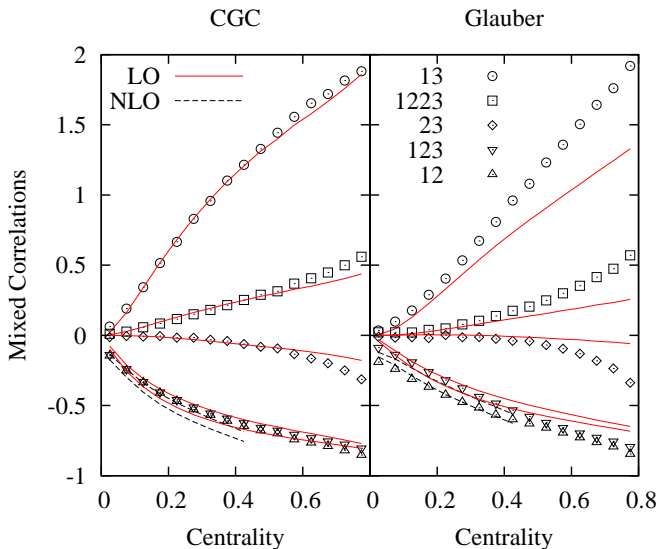


FIG. 3. (Color online) Mixed correlations versus centrality. From top to bottom: $\varepsilon_{13}/(\varepsilon_1\{2\}^3\varepsilon_3\{2\})$ (labeled 13), $\varepsilon_{1223}/(\varepsilon_1\{2\}\varepsilon_2\{2\}^2\varepsilon_3\{2\})$ (labeled 1223), $\varepsilon_{23}/(\varepsilon_2\{2\}^3\varepsilon_3\{2\}^2)$ (labeled 23), $\varepsilon_{123}/(\varepsilon_1\{2\}\varepsilon_2\{2\}\varepsilon_3\{2\})$ (labeled 123) and $\varepsilon_{12}/(\varepsilon_1\{2\}^2\varepsilon_2\{2\})$ (labeled 12). Symbols are Monte-Carlo results. Full lines are analytic results to leading-order in $1/N$. Dashed lines for ε_{12} and ε_{123} include next-to-leading order corrections derived in Appendix. As in Fig. 2, we display NLO results up to 40% centrality, although they are only valid for central collisions.

Φ_1 is more likely to be perpendicular to the participant plane. Because of the strong correlation between $3\Phi_1$ and $3\Phi_3$, this also explains why the mixed correlation ε_{123} is also negative [15, 17].

A closer look at Fig. 3 reveals that our leading-order results for ε_{12} and ε_{123} do not agree well with Monte-Carlo for central collisions, where both ratios are small but not zero, while our leading-order results go smoothly to zero. Agreement is improved by including the next-to-leading term, which is of order $1/N^2$, negative, and does not vanish for central collisions. This term is calculated in the Appendix for central collisions.

V. CONCLUSIONS

We have shown that the magnitude of initial-state anisotropies ε_n , their fluctuations and mutual correlations can be understood within a simple model where fluctuations stem from identical, independent sources, which can be viewed as “hot spots” scattered across the interaction region [46, 47]. The independent-source model reproduces results from both CGC-inspired and Glauber Monte-Carlo models.

In our model, all information about the initial state is encoded in a few parameters: the number of sources N , the profile of a single source, and the distribution of

sources across the transverse plane. We have considered pointlike sources for simplicity. The magnitudes of ε_3 and ε_1 show that N is roughly half the number of participant nucleons, which means that participant nucleons are correlated pairwise. The angular correlations between Φ_1 , Φ_2 and Φ_3 are independent of N to leading order in $1/N$. They only depend on the distribution of sources, and are mostly driven by the almond shape of the overlap area between the two nuclei, which is responsible for the large elliptic flow [48].

There is an ambiguity in the definition of the “initial state”. What is computed in Monte-Carlo models (KLN or Glauber) is typically the distribution of energy right after the nuclei have passed through each other. On the other hand, the relevant anisotropies for collective flow are the anisotropies at a somewhat later time, when the system reaches local equilibrium. The value of ε_n decreases during this thermalization time [28]. We have shown that this decrease is solely due to the increase in the system size, due to the smearing of each source. ε_3 depends more strongly on the system size than ε_2 , which explains why it decreases more strongly during the thermalization phase. (This effect was interpreted by the authors of Ref. [28] as an interference between ε_2 and ε_3 .)

Within our independent-source model, ratios such as $\langle\varepsilon_n^4\rangle/\langle\varepsilon_n^2\rangle^2$, as well as the various angular correlations between event planes considered in [18], are independent of the number of sources to leading order in $1/N$ (with the exception of $\langle\varepsilon_2^4\rangle/\langle\varepsilon_2^2\rangle^2$). Remarkably, these ratios are also unchanged through the early-time dynamics, and are therefore well-defined observables for initial-state fluctuations.

ACKNOWLEDGMENTS

We would like to thank Clément Gombeaud for help with the Monte-Carlo models, and in particular for providing the code for centrality determination. This work is funded by “Agence Nationale de la Recherche” under grant ANR-08-BLAN-0093-01 and by CEFIPRA under project 4404-2. RSB acknowledges the hospitality of IPhT Saclay where part of this work was done.

Appendix A: Higher-order calculations

In this Appendix, we present next-to-leading order calculations in $1/N$ for a few moments. Since next-to-leading order calculations are considerably more involved than leading-order calculations, we assume azimuthal symmetry for sake of simplicity. We compute three quantities for which our leading-order results vanish in the limit of azimuthal symmetry, namely, $\varepsilon_3\{4\}$, ε_{12} and ε_{123} .

We first compute $\varepsilon_3\{4\}$. Taking the recentering cor-

rection into account, the expression of ε_3 is

$$\varepsilon_3^2 = \frac{\{(z - \delta_z)^3\}\{(\bar{z} - \delta_{\bar{z}})^3\}}{\{|z - \delta_z|^3\}^2}. \quad (\text{A1})$$

Treating δ as the expansion parameter, we can expand this expression to any desired order in δ . For instance, $\{(z - \delta_z)^3\} = \delta_{z^3} - 3\langle z^2 \rangle \delta_z - 3\delta_{z^2} \delta_z + 2(\delta_z)^3$. We organize the calculation as follows. Let

$$\varepsilon_3^2 = B + C + D + \dots, \quad (\text{A2})$$

where $B \sim \mathcal{O}(\delta^2)$, $C \sim \mathcal{O}(\delta^3)$, etc. (There are no terms independent of δ or of order δ .) Hence

$$\varepsilon_3\{2\}^2 \equiv \langle \varepsilon_3^2 \rangle = \langle B \rangle + \langle C \rangle + \langle D \rangle + \dots, \quad (\text{A3})$$

and

$$\begin{aligned} \varepsilon_3\{4\}^4 &\equiv 2\langle \varepsilon_3^2 \rangle^2 - \langle \varepsilon_3^4 \rangle \\ &= 2\langle B \rangle^2 - \langle B^2 \rangle \\ &\quad + 2\langle C \rangle^2 - \langle C^2 \rangle \\ &\quad + 2\langle D \rangle^2 - \langle D^2 \rangle \\ &\quad + 4\langle B \rangle \langle C \rangle - 2\langle BC \rangle \\ &\quad + 4\langle B \rangle \langle D \rangle - 2\langle BD \rangle \\ &\quad + 4\langle C \rangle \langle D \rangle - 2\langle CD \rangle + \dots. \end{aligned} \quad (\text{A4})$$

To proceed further, we make use of the expressions for $\langle \delta_f \delta_g \rangle$, $\langle \delta_f \delta_g \delta_h \rangle$, $\langle \delta_f \delta_g \delta_h \delta_u \rangle$, $\langle \delta_f \delta_g \delta_h \delta_u \delta_v \rangle$ and $\langle \delta_f \delta_g \delta_h \delta_u \delta_v \delta_w \rangle$ given in [43]. (These expressions ignore correlations between participant positions.) Dominant terms in these five quantities are of $\mathcal{O}(1/N)$, $\mathcal{O}(1/N^2)$, $\mathcal{O}(1/N^2)$, $\mathcal{O}(1/N^3)$ and $\mathcal{O}(1/N^3)$, respectively, where N is the number of participants. For central collisions, azimuthal symmetry allows to simplify the previous expression:

$$\varepsilon_3\{4\}^4 = 2\langle B \rangle^2 - \langle B^2 \rangle - \langle C^2 \rangle + 4\langle B \rangle \langle C \rangle - 2\langle BC \rangle + 4\langle B \rangle \langle D \rangle - 2\langle BD \rangle. \quad (\text{A5})$$

After some algebra, we get

$$\varepsilon_3\{4\}^4 = \frac{1}{N^3} \left[\frac{2\langle r^6 \rangle^2 - \langle r^{12} \rangle}{\langle r^3 \rangle^4} + \frac{8\langle r^6 \rangle \langle r^9 \rangle}{\langle r^3 \rangle^5} - \frac{8\langle r^6 \rangle^3}{\langle r^3 \rangle^6} \right]. \quad (\text{A6})$$

A similar result has been derived previously for $\varepsilon_2\{4\}^4$, which is also of order $1/N^3$ for independent sources and central collisions [43]. This scaling in $1/N^3$ is natural for the four-particle cumulant [31].

Other moments can be computed in a similar way. Our results for ε_{123} and ε_{12} are given in Appendix B.

Appendix B: Summary of results

The expressions of $\varepsilon_n\{2\}^2$ to order $1/N$ are given by Eqs. (11) and (12). The higher-order cumulant $\varepsilon_1\{4\}^4$ has been derived to order $1/N^2$:

$$\varepsilon_1\{4\}^4 \equiv 2\langle \varepsilon_1^2 \rangle^2 - \langle \varepsilon_1^4 \rangle$$

$$= -\frac{1}{N^2 \langle r^3 \rangle^4} [\langle r^6 \cos 2\phi \rangle - 8\varepsilon_s \langle r^2 \rangle^3 + 2\varepsilon_s \langle r^2 \rangle \langle r^4 \rangle - 4\langle r^2 \rangle \langle r^4 \cos 2\phi \rangle - \varepsilon_s^3 \langle r^2 \rangle^3]^2. \quad (\text{B1})$$

The expression of $\varepsilon_2\{4\}^4$ was derived in [43] up to order $1/N^3$ for central collisions:

$$\begin{aligned} \varepsilon_2\{4\}^4 &\equiv 2\langle \varepsilon_2^2 \rangle^2 - \langle \varepsilon_2^4 \rangle \\ &= \varepsilon_s^4 + \frac{1}{N \langle r^2 \rangle^2} [2\varepsilon_s^4 \langle r^4 \rangle - 2\varepsilon_s^2 \langle r^4 \cos 4\phi \rangle] \\ &\quad + \frac{1}{N^2} \left[8\varepsilon_s^2 \frac{\langle r^6 \rangle}{\langle r^2 \rangle^3} + 4\varepsilon_s \frac{\langle r^6 \cos 2\phi \rangle}{\langle r^2 \rangle^3} \right. \\ &\quad \left. - 16\varepsilon_s^2 \frac{\langle r^4 \rangle^2}{\langle r^2 \rangle^4} - 16\varepsilon_s \frac{\langle r^4 \rangle \langle r^4 \cos 2\phi \rangle}{\langle r^2 \rangle^4} \right] \\ &\quad + \frac{1}{N^3} \left[\frac{2\langle r^4 \rangle^2}{\langle r^2 \rangle^4} - \frac{\langle r^8 \rangle}{\langle r^2 \rangle^4} + \frac{8\langle r^4 \rangle \langle r^6 \rangle}{\langle r^2 \rangle^5} \right. \\ &\quad \left. - \frac{8\langle r^4 \rangle^3}{\langle r^2 \rangle^6} \right] \end{aligned} \quad (\text{B2})$$

Our result for $\varepsilon_3\{4\}^4$ to order $1/N^3$ is

$$\begin{aligned} \varepsilon_3\{4\}^4 &\equiv 2\langle \varepsilon_3^2 \rangle^2 - \langle \varepsilon_3^4 \rangle \\ &= -\frac{1}{N^2 \langle r^3 \rangle^4} [\langle r^6 \cos 6\phi \rangle + 6\varepsilon_s \langle r^2 \rangle \langle r^4 \cos 4\phi \rangle \\ &\quad - 9\varepsilon_s^3 \langle r^2 \rangle^3]^2 \\ &\quad + \frac{1}{N^3 \langle r^3 \rangle^4} \left[2\langle r^6 \rangle^2 - \langle r^{12} \rangle + \frac{8\langle r^6 \rangle \langle r^9 \rangle}{\langle r^3 \rangle} \right. \\ &\quad \left. - \frac{8\langle r^6 \rangle^3}{\langle r^3 \rangle^2} \right]. \end{aligned} \quad (\text{B3})$$

The 3-point mixed correlations are, to order $1/N^2$,

$$\begin{aligned} \varepsilon_{12} &= \frac{\varepsilon_s}{N \langle r^3 \rangle^2} [\langle r^6 \cos 2\phi \rangle - 8\varepsilon_s \langle r^2 \rangle^3 + 2\varepsilon_s \langle r^2 \rangle \langle r^4 \rangle \\ &\quad - 4\langle r^2 \rangle \langle r^4 \cos 2\phi \rangle - \varepsilon_s^3 \langle r^2 \rangle^3] \\ &\quad + \frac{1}{N^2} \left[\frac{4\langle r^4 \rangle^2 - \langle r^8 \rangle}{\langle r^2 \rangle \langle r^3 \rangle^2} \right. \\ &\quad \left. + \frac{8\langle r^2 \rangle^3 + 4\langle r^6 \rangle - 16\langle r^2 \rangle \langle r^4 \rangle}{\langle r^3 \rangle^2} \right], \end{aligned} \quad (\text{B4})$$

and

$$\begin{aligned} \varepsilon_{123} &= \frac{\varepsilon_s}{N \langle r^3 \rangle^2} [\langle r^6 \cos 2\phi \rangle + 3\varepsilon_s \langle r^2 \rangle \langle r^4 \rangle - 6\varepsilon_s \langle r^2 \rangle^3 \\ &\quad - 3\varepsilon_s^3 \langle r^2 \rangle^3 - 2\langle r^2 \rangle \langle r^4 \cos 2\phi \rangle \\ &\quad + \varepsilon_s \langle r^2 \rangle \langle r^4 \cos 4\phi \rangle] \\ &\quad + \frac{1}{N^2} \left[\frac{2\langle r^6 \rangle - 6\langle r^2 \rangle \langle r^4 \rangle}{\langle r^3 \rangle^2} + \frac{3\langle r^4 \rangle^2 - \langle r^8 \rangle}{\langle r^2 \rangle \langle r^3 \rangle^2} \right] \end{aligned} \quad (\text{B5})$$

For higher-order mixed correlations, we have only carried out leading-order calculations. The 4-point correlations considered in this paper are

$$\begin{aligned} \varepsilon_{1223} &= \frac{\varepsilon_s^2}{N \langle r^3 \rangle^2} [\langle r^6 \cos 4\phi \rangle + 4\varepsilon_s \langle r^2 \rangle \langle r^4 \cos 2\phi \rangle \\ &\quad - 2\langle r^2 \rangle \langle r^4 \cos 4\phi \rangle + 9\varepsilon_s^2 \langle r^2 \rangle^3] \end{aligned} \quad (\text{B6})$$

and

$$\begin{aligned} \varepsilon_{13} = & \frac{3}{N^2 \langle r^3 \rangle^4} \left[\langle r^6 \cos 2\phi \rangle - 8\varepsilon_s \langle r^2 \rangle^3 + 2\varepsilon_s \langle r^2 \rangle \langle r^4 \rangle \right. \\ & \left. - 4\langle r^2 \rangle \langle r^4 \cos 2\phi \rangle - \varepsilon_s^3 \langle r^2 \rangle^3 \right] \\ & \times \left[\langle r^6 \cos 2\phi \rangle + 3\varepsilon_s \langle r^2 \rangle \langle r^4 \rangle - 6\varepsilon_s \langle r^2 \rangle^3 \right. \\ & \left. - 3\varepsilon_s^3 \langle r^2 \rangle^3 - 2\langle r^2 \rangle \langle r^4 \cos 2\phi \rangle \right. \\ & \left. + \varepsilon_s \langle r^2 \rangle \langle r^4 \cos 4\phi \rangle \right]. \end{aligned} \quad (\text{B7})$$

Finally, we have computed the 5-point correlation

$$\begin{aligned} \varepsilon_{23} = & \frac{\varepsilon_s^3}{N \langle r^3 \rangle^2} \left[\langle r^6 \cos 6\phi \rangle + 6\varepsilon_s \langle r^2 \rangle \langle r^4 \cos 4\phi \rangle \right. \\ & \left. - 9\varepsilon_s^3 \langle r^2 \rangle^3 \right]. \end{aligned} \quad (\text{B8})$$

For sake of completeness, we list all other 4- and 5-point correlations which can be constructed out of the first three harmonics, and their expressions to leading order,

obtained using Wick's theorem:

$$\begin{aligned} \varepsilon\{2, -2, 3, -3\} &= \varepsilon_2 \{2\}^2 \varepsilon_3 \{2\}^2 \\ \varepsilon\{1, -1, 2, -2\} &= \varepsilon_1 \{2\}^2 \varepsilon_2 \{2\}^2 \\ \varepsilon\{1, -1, 3, -3\} &= \varepsilon_1 \{2\}^2 \varepsilon_3 \{2\}^2 + \varepsilon\{3, 1\}^2 + \varepsilon\{3, -1\}^2 \\ \varepsilon\{1, 2, 3, -3\} &= \varepsilon_s (2\varepsilon_3 \{2\}^2 \varepsilon\{3, -1\} + \varepsilon\{3, 1\} \varepsilon\{3, 3\}) \\ \varepsilon\{1, 1, -1, 2, -3\} &= \varepsilon_s (2\varepsilon_1 \{2\}^2 \varepsilon\{3, -1\} + \varepsilon\{1, 1\} \varepsilon\{3, 1\}) \\ \varepsilon\{1, 1, -2, 3, -3\} &= \varepsilon_s (2\varepsilon\{3, 1\} \varepsilon\{3, -1\} + \varepsilon_3 \{2\}^2 \varepsilon\{1, 1\}) \\ \varepsilon\{1, 2, 2, -2, -3\} &= \varepsilon_2 \{2\}^2 \varepsilon_{123} \\ \varepsilon\{1, 1, 2, -2, -2\} &= \varepsilon_2 \{2\}^2 \varepsilon_{12} \\ \varepsilon\{1, 1, 1, -1, -2\} &= 3\varepsilon_1 \{2\}^2 \varepsilon_{12}. \end{aligned} \quad (\text{B9})$$

The first of these equations means that there are no correlations between the magnitudes of ε_2 and ε_3 to leading order. This could be tested experimentally by measuring the correlation between the magnitudes of v_2 and v_3 .

-
- [1] C. E. Aguiar, Y. Hama, T. Kodama and T. Osada, Nucl. Phys. A **698**, 639 (2002) [arXiv:hep-ph/0106266].
- [2] S. Mrowczynski and E. V. Shuryak, Acta Phys. Polon. B **34**, 4241 (2003) [arXiv:nucl-th/0208052].
- [3] M. Miller and R. Snellings, arXiv:nucl-ex/0312008.
- [4] B. Alver *et al.* [PHOBOS Collaboration], Phys. Rev. Lett. **98**, 242302 (2007) [arXiv:nucl-ex/0610037].
- [5] J. Casalderrey-Solana, U. A. Wiedemann, Phys. Rev. Lett. **104**, 102301 (2010). [arXiv:0911.4400 [hep-ph]].
- [6] E. Avsar, C. Flensburg, Y. Hatta, J. -Y. Ollitrault, T. Ueda, Phys. Lett. **B702**, 394-397 (2011). [arXiv:1009.5643 [hep-ph]].
- [7] P. Bozek, Eur. Phys. J. **C71**, 1530 (2011). [arXiv:1010.0405 [hep-ph]].
- [8] K. Werner, I. Karpenko, T. Pierog, Phys. Rev. Lett. **106**, 122004 (2011). [arXiv:1011.0375 [hep-ph]].
- [9] V. Khachatryan *et al.* [CMS Collaboration], JHEP **1009**, 091 (2010). [arXiv:1009.4122 [hep-ex]].
- [10] M. Luzum, Phys. Lett. B **696**, 499 (2011) [arXiv:1011.5773 [nucl-th]].
- [11] M. Luzum, [arXiv:1107.0592 [nucl-th]].
- [12] B. Alver and G. Roland, Phys. Rev. C **81**, 054905 (2010) [Erratum-ibid. C **82**, 039903 (2010)] [arXiv:1003.0194 [nucl-th]].
- [13] A. Adare *et al.* [PHENIX Collaboration], [arXiv:1105.3928 [nucl-ex]].
- [14] K. Aamodt *et al.* [ALICE Collaboration], Phys. Rev. Lett. **107**, 032301 (2011). [arXiv:1105.3865 [nucl-ex]].
- [15] D. Teaney and L. Yan, Phys. Rev. C **83**, 064904 (2011) [arXiv:1010.1876 [nucl-th]].
- [16] M. Luzum, J. -Y. Ollitrault, Phys. Rev. Lett. **106**, 102301 (2011). [arXiv:1011.6361 [nucl-ex]].
- [17] P. Staig and E. Shuryak, arXiv:1008.3139 [nucl-th].
- [18] R. S. Bhalerao, M. Luzum, J. -Y. Ollitrault, Phys. Rev. **C84**, 034910 (2011). [arXiv:1104.4740 [nucl-th]].
- [19] R. Andrade, F. Grassi, Y. Hama, T. Kodama and O. J. Socolowski, Phys. Rev. Lett. **97**, 202302 (2006) [arXiv:nucl-th/0608067].
- [20] H. Petersen, G. Y. Qin, S. A. Bass and B. Muller, Phys. Rev. C **82**, 041901 (2010) [arXiv:1008.0625 [nucl-th]].
- [21] K. Werner, K. Mikhailov, Iu. Karpenko, T. Pierog, [arXiv:1104.2405 [hep-ph]].
- [22] J. Xu and C. M. Ko, Phys. Rev. C **83**, 021903 (2011) [arXiv:1011.3750 [nucl-th]].
- [23] J. Xu, C. M. Ko, Phys. Rev. **C84**, 014903 (2011). [arXiv:1103.5187 [nucl-th]].
- [24] W. Broniowski, P. Bozek and M. Rybczynski, Phys. Rev. C **76**, 054905 (2007) [arXiv:0706.4266 [nucl-th]].
- [25] B. Schenke, S. Jeon and C. Gale, Phys. Rev. Lett. **106**, 042301 (2011) [arXiv:1009.3244 [hep-ph]].
- [26] R. S. Bhalerao and J. Y. Ollitrault, Phys. Lett. B **641**, 260 (2006) [arXiv:nucl-th/0607009].
- [27] H. Holopainen, H. Niemi and K. J. Eskola, Phys. Rev. C **83**, 034901 (2011) [arXiv:1007.0368 [hep-ph]].
- [28] G. Y. Qin, H. Petersen, S. A. Bass and B. Muller, Phys. Rev. C **82**, 064903 (2010) [arXiv:1009.1847 [nucl-th]].
- [29] F. G. Gardim, F. Grassi, Y. Hama, M. Luzum, J. -Y. Ollitrault, Phys. Rev. **C83**, 064901 (2011). [arXiv:1103.4605 [nucl-th]].
- [30] Z. Qiu, U. W. Heinz, Phys. Rev. **C84**, 024911 (2011). [arXiv:1104.0650 [nucl-th]].
- [31] N. Borghini, P. M. Dinh and J. Y. Ollitrault, Phys. Rev. C **64**, 054901 (2001) [arXiv:nucl-th/0105040].
- [32] Code by A. Dumitru, a fork of MC-KLN by Y. Nara. Version 1.00 obtained from http://physics.baruch.cuny.edu/files/CGC/CGC_IC.html
- [33] H. J. Drescher and Y. Nara, Phys. Rev. C **76**, 041903 (2007) [arXiv:0707.0249 [nucl-th]].
- [34] J. L. Albacete and A. Dumitru, arXiv:1011.5161 [hep-ph].
- [35] M. L. Miller, K. Reygers, S. J. Sanders, P. Steinberg, Ann. Rev. Nucl. Part. Sci. **57**, 205-243 (2007). [nucl-ex/0701025].
- [36] C. Gombeaud, J. -Y. Ollitrault, J. Phys. G **G37**, 094024 (2010). [arXiv:0912.3623 [nucl-th]].
- [37] P. Bozek, M. Chojnacki, W. Florkowski, B. Tomasik, Phys. Lett. **B694**, 238-241 (2010). [arXiv:1007.2294 [nucl-th]].
- [38] B. Alver, M. Baker, C. Loizides and P. Steinberg, arXiv:0805.4411 [nucl-ex].

- [39] T. Hirano, U. W. Heinz, D. Kharzeev, R. Lacey, Y. Nara, Phys. Lett. **B636**, 299-304 (2006). [nucl-th/0511046].
- [40] T. Lappi, R. Venugopalan, Phys. Rev. **C74**, 054905 (2006). [nucl-th/0609021].
- [41] K. Aamodt *et al.* [The ALICE Collaboration], Phys. Rev. Lett. **105**, 252302 (2010). [arXiv:1011.3914 [nucl-ex]].
- [42] S. A. Voloshin, A. M. Poskanzer, A. Tang and G. Wang, Phys. Lett. B **659**, 537 (2008) [arXiv:0708.0800 [nucl-th]].
- [43] B. Alver *et al.*, Phys. Rev. C **77**, 014906 (2008) [arXiv:0711.3724 [nucl-ex]].
- [44] R. S. Bhalerao, M. Luzum, J. -Y. Ollitrault, [arXiv:1106.4940 [nucl-ex]].
- [45] J. L. Nagle and M. P. McCumber, Phys. Rev. C **83**, 044908 (2011) [arXiv:1011.1853 [nucl-ex]].
- [46] M. Gyulassy, D. H. Rischke, B. Zhang, Nucl. Phys. **A613**, 397-434 (1997) [nucl-th/9609030].
- [47] G. -L. Ma, X. -N. Wang, Phys. Rev. Lett. **106**, 162301 (2011). [arXiv:1011.5249 [nucl-th]].
- [48] J. -Y. Ollitrault, Phys. Rev. **D46**, 229-245 (1992).